

Article

# Approximate Explicit Solution to the Green-Ampt Infiltration Model for Estimating Wetting Front Depth

Wei-Bo Nie <sup>1</sup>, Yi-Bo Li <sup>2</sup>, Liang-Jun Fei <sup>1</sup> and Xiao-Yi Ma <sup>2,\*</sup>

<sup>1</sup> State Key Laboratory Base of Eco-hydraulic Engineering in Arid Area, Xi'an University of Technology, Xi'an 710048, China; nwbo2000@163.com (W.-B.N.); feiliangjun2008@163.com (L.-J.F.)

<sup>2</sup> College of Water Resources and Architectural Engineering, Northwest A & F University, Yangling 712100, China; liyibo51\_teresa@hotmail.com

\* Correspondence: xma@nwfufu.edu.cn; Tel.: +86-29-8708-2860

Received: 10 July 2017; Accepted: 9 August 2017; Published: 22 August 2017

**Abstract:** Obtaining reliable information on the wetting front depth of soil is beneficial to the understanding of one-dimensional (1D) vertical infiltration under border irrigation. This paper presents an approximate explicit solution to the Green-Ampt (GA) infiltration model for estimating the wetting front depth. Moreover, the model proposed in this study, the GA model, the Ali model, and the Stone model were validated and evaluated using laboratory experimental data and HYDRUS-1D simulation. Statistical comparisons (root mean square error-RMSE, mean absolute percent relative error-MAPRE, and percent bias-PB) of the estimated data with the measured and simulated data were conducted. The models were ranked on the basis of their overall performance index (OPI). The results demonstrated that all four models can be used to estimate the wetting front depth of 1D vertical infiltration for a wide range of soil textures; the proposed model provided the most accurate result. According to comparisons of the estimated values with the measured and simulated values, the maximum RMSE, MAPRE, and PB were 1.74 cm, 6.92%, and  $-6.74\%$ , respectively, for the proposed model. On the basis of the OPI, the optimal model was the proposed model, followed by the Ali, GA, and Stone models.

**Keywords:** Green-Ampt; explicit equation; wetting front; vertical infiltration

## 1. Introduction

Border irrigation is one of the main irrigation methods used in China. Obtaining reliable information on the wetting front depth of soil is beneficial for a comprehensive understanding of the one-dimensional (1D) infiltration process under border irrigation. However, directly measuring the wetting front depth of soil in a field under irrigation is difficult. Thus, previous studies have developed several different models to estimate the wetting front depth of soil empirically and physically [1,2]. The empirical models are usually derived on the basis of field or laboratory experimental data [3] or on a simple equation [1,4–6] under specific conditions, and so a method that can fully describe the advancement of the wetting front process and that can be used universally is unavailable. However, the physically based models describe the infiltration process in detail, and Richards's model and the Green-Ampt (GA) model are those most commonly used for simulating the infiltration process. The solution to Richards's model requires an iterative implicit numerical technique with fine discretization in time and space; thus, this model is computationally intensive [7–10]. The GA model [11] is an analytical solution derived from Darcy's equation and is derived indirectly through Richards's model with some simplification [12]. Because of its simplicity and accuracy, several modifications of the GA model have been widely used to simulate the 1D vertical infiltration of water into soil.

The GA model assumes that a sharp wetting front separates the soil profile into an upper saturated zone and a lower unsaturated zone. The model is essentially an equation in which an algebraic and logarithmic term is used to implicitly represent the time-varying cumulative infiltration volume [2,13]. In the GA model, the cumulative infiltration volume is estimated using an iteration method [7,13,14]. To avoid performing iterations, different forms of explicit solutions to the GA model have been developed [13,15–22]. Each approximation has its own merits and demerits in terms of its relative complexity and errors for estimating the cumulative infiltration volume. However, few studies have focused on estimating the wetting front advancement depth of 1D vertical infiltration by deriving explicit solutions to the GA model. Stone et al. [13] expressed the GA model by using the first two terms of a Taylor series expansion of the equation, with a term added to account for the error in the approximation. In the Stone model, it is assumed that the steady infiltration rate is equal to the saturated conductivity, which is inconsistent with the actual conditions [23–26]; thus, this assumption may reduce the accuracy of the model for estimating the wetting front depth. Ali et al. [27] replaced the logarithmic term of the GA model by a sequential segmental second-order polynomial, producing explicit equation-based models for estimating the wetting front depth of 1D vertical infiltration, and the maximum relative error obtained between the approximation and the GA model was 0.5%. However, model parameters must be selected according to different infiltration segments; thus, applying the Ali model is complex. According to a review of the literature, selecting the most accurate and reliable approximate solution to the GA model for estimating the wetting front advancement depth is difficult, and the existing approximate explicit GA models for estimating the wetting front of 1D vertical infiltration have not been evaluated.

Therefore, the objectives of this study were: (1) to propose an approximate explicit solution to the GA model for estimating the wetting front depth of 1D vertical infiltration, and (2) to validate and evaluate the model proposed in this study—in addition to the GA model, the Ali model, and the Stone model—by using laboratory experimental data and HYDRUS-1D simulations.

## 2. Model Description

### 2.1. GA Model

The GA model is based on the assumption that the soil surface is continuously wetted by ponding water during infiltration, and the wetted and dry regions of the wetting domain are assumed to be separated by a sharp wetting front. Under these conditions, the GA infiltration model can be written as [28]

$$i = K_s \left( 1 + \frac{h_0 + \psi_m}{Z_f} \right) \quad (1)$$

where  $i$  is the infiltration rate per unit area at a given time ( $\text{cm min}^{-1}$ ),  $K_s$  represents the saturated conductivity ( $\text{cm min}^{-1}$ ),  $Z_f$  is the depth of the advancement of the wetting front (cm),  $h_0$  is the depth of the ponding water (cm), and  $\psi_m$  is the suction head at the wetting front (cm). The variable  $\psi_m$  is estimated by subtracting the hydraulic conductivity from the weighted average of the soil pressure head, and this solution was proposed by Bautista et al. [29]. Under ponding water conditions, the cumulative infiltration volume can be written as [28]

$$I = Z_f \Delta\theta \quad (2)$$

where  $I$  is the cumulative infiltration volume per unit area (cm) and  $\Delta\theta$  is the fillable porosity, which can be calculated using the following formula:  $\theta_s - \theta_0$ , in which  $\theta_0$  is the initial volumetric moisture content ( $\text{cm}^3 \text{cm}^{-3}$ ) and  $\theta_s$  is the saturation moisture content ( $\text{cm}^3 \text{cm}^{-3}$ ). Substituting Equation (2) into Equation (1), for a constant  $h_0$ , and by replacing  $i$  with  $dI/dt$ , Equation (1) after integration can be expressed as

$$I = K_s t + (h_0 + \psi_m) \Delta\theta \left[ \ln \left( 1 + \frac{I}{(h_0 + \psi_m) \Delta\theta} \right) \right] \quad (3)$$

where  $t$  is the infiltration time (min). Substituting Equation (2) into Equation (3), Equation (3) becomes

$$Z_f = \frac{K_s t}{\Delta\theta} + (h_0 + \psi_m) \left[ \ln \left( 1 + \frac{Z_f}{h_0 + \psi_m} \right) \right] \quad (4)$$

Equation (4) is another form of the GA implicit infiltration model, and it can be solved to estimate the depth of the advancement of the wetting front,  $Z_f$ , for increments in time by using any suitable iterative scheme [7,13,14].

## 2.2. Stone Model

Two common dimensionless infiltration variables—namely the dimensionless infiltration time,  $T^*$ , and the dimensionless depth of the advancement of the wetting front,  $L^*$ —are defined as follows:

$$T^* = \frac{K_s t}{(h_0 + \psi_m) \Delta\theta} \quad (5)$$

$$L^* = \frac{I}{(h_0 + \psi_m) \Delta\theta} = \frac{Z_f}{h_0 + \psi_m} \quad (6)$$

Substituting Equations (5) and (6) into Equation (4), the dimensionless form of Equation (4) can be expressed as

$$T^* = L^* - \ln(1 + L^*) \quad (7)$$

Stone et al. [13] developed an alternative approximation to Equation (7) by rewriting it in the form of Philip's model [30] and by adding an error term to Equation (7) to account for the approximation deviation. The resulting approximation of Equation (7) can be written as

$$L^* = T^* + (2 \times T^*)^{0.5} - 0.2978 T^{*0.7913} \quad (8)$$

Returning to the original variables, Equation (8) becomes

$$Z_f = \frac{K_s t}{\Delta\theta} + \sqrt{\frac{2K_s(h_0 + \psi_m)t}{\Delta\theta}} - 0.2978 \left[ \frac{K_s(h_0 + \psi_m)^{0.264} t}{\Delta\theta} \right]^{0.7913} \quad (9)$$

## 2.3. Ali Model

Ali et al. [27] developed a generalized explicit model for estimating the time-varying depth of the advancement of the wetting front,  $Z_f$ , by replacing the logarithmic term in Equation (4) with sequential segmental second-order polynomials. The derived explicit model for the wetting front depth is as follows [27]:

$$Z_f = (h_0 + \psi_m) \left[ \sqrt{\frac{F_1 K_s}{(h_0 + \psi_m) \Delta\theta} t} + F_2 + F_3 \right] \quad (10)$$

where  $F_1$ ,  $F_2$ , and  $F_3$  are the model coefficients for different ranges of the dimensionless depth of the wetting front. The numerical parameters of Equation (10),  $F_1$ ,  $F_2$  and  $F_3$ , are taken from the study by Ali et al. [27];  $Z_f$  is computed from Equation (10) by using the respective segmental values of the numerical factors,  $F_1$ ,  $F_2$  and  $F_3$ , satisfying the dimensionless  $L^*$  conditions (Equation (6)).

## 2.4. Proposed Model

To describe the 1D vertical infiltration process, Valiantzas [31] proposed a new two-parameter infiltration equation based on Philip's model [30]. The functional form is as follows:

$$I \cong 0.5K_s t + S\sqrt{t} \left[ 1 + \left( \frac{0.5K_s}{S} \right)^2 t \right]^{0.5} \quad (11)$$

where  $S$  is the sorptivity ( $\text{cm min}^{-0.5}$ ), which can be written as [28]

$$S = \sqrt{2K_s(h_0 + \psi_m)\Delta\theta} \quad (12)$$

Substituting Equation (2) and Equation (12) into Equation (11), Equation (11) becomes

$$Z_f\Delta\theta \cong 0.5K_s t + \sqrt{2K_s(h_0 + \psi_m)\Delta\theta t} \left[1 + \frac{K_s t}{8(h_0 + \psi_m)\Delta\theta}\right]^{0.5} \quad (13)$$

Substituting Equations (5) and (6) into Equation (13), Equation (13) can be written as

$$L^* \cong 0.5T^* + \sqrt{2T^*} \left[1 + \frac{T^*}{8}\right]^{0.5} \quad (14)$$

Similarly to Stone et al. [13], an error term is included in Equation (14) to account for the approximation. Subsequently, Equation (14) can be written as

$$L^* = 0.5T^* + \sqrt{2T^*} \left[1 + \frac{T^*}{8}\right]^{0.5} + \varepsilon \quad (15)$$

where  $\varepsilon$  is the error term. Generally, the root zone is less than 100 cm deep during crop growth. Thus, for a high irrigation performance, the depth of the wetting front  $Z_f$  should match the depth of the root zone. Considering the actual situation, it is reasonable to assume that the maximum  $Z_f$  is 100 cm under surface irrigation. Moreover, the water depth,  $h_0$ , usually ranges from 5 to 10 cm under surface irrigation [32,33], and the value of the suction head,  $\psi_m$ , is a nonnegative number in the GA model (Equation (1)). Thus, on the basis of all the aforementioned analyses, the maximum value of  $L^*$  is less than 20, according to Equation (6). The range for  $L^*$  of between 0 and 20, which was adopted by Stone et al. [13], was also employed in this study. Figure 1 depicts the dimensionless  $T^*$  versus  $L^*$  according to Equation (7). The error term can be calculated by substituting the  $T^*$  and  $L^*$  values illustrated in Figure 1 into Equation (15). Figure 2 presents the dimensionless  $\varepsilon$  versus  $T^*$ .

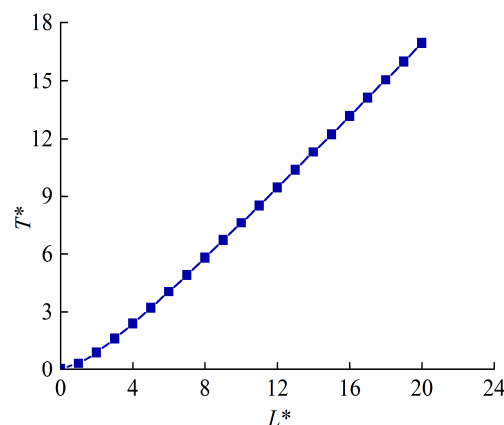


**Figure 1.** Representation of dimensionless infiltration time ( $T^*$ ) versus dimensionless depth of the advancement of the wetting front ( $L^*$ ) according to Equation (7).

As displayed in Figure 2, the portion of the single relationship of  $\varepsilon$  versus  $T^*$  can be approximated using a least-square curve fitting technique by substituting the power term [13]. Regarding the goodness of fit between the dimensionless  $\varepsilon$  versus  $T^*$ , the coefficient of determination ( $R^2$ ) from the regressions was 0.993 for the range of  $L^*$  between 0 and 20. Substituting the power term of Figure 2 into Equation (15), Equation (15) can be written as

$$L^* = 0.5T^* + \sqrt{2T^*} \left[ 1 + \frac{T^*}{8} \right]^{0.5} + 0.1461T^{*0.788} \tag{16}$$

Returning to the original variables, Equation (16) becomes

$$Z_f = \frac{0.5K_s t}{\Delta\theta} + \sqrt{\frac{2K_s(h_0 + \psi_m)t}{\Delta\theta}} \left[ 1 + \frac{K_s t}{8(h_0 + \psi_m)\Delta\theta} \right]^{0.5} + 0.1461 \left[ \frac{K_s(h_0 + \psi_m)^{0.269} t}{\Delta\theta} \right]^{0.788} \tag{17}$$

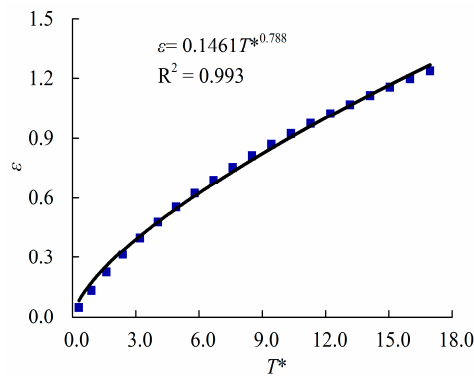


**Figure 2.** Representation of dimensionless error term ( $\varepsilon$ ) versus dimensionless infiltration time ( $T^*$ ) according to Equation (15).

### 3. Materials and Methods

#### 3.1. Laboratory Experiment

Laboratory experimental data were used to evaluate the four models explained in Section 2. The two data sets presented by Fok and Chiang [34] for Makiki clay under different initial soil moisture levels (i.e., dry and wet) were used in this study. For dry soil samples,  $K_s$ ,  $h_0 + \psi_m$ , and  $\Delta\theta$  were taken as  $0.0039 \text{ cm min}^{-1}$ ,  $69.3 \text{ cm}$ , and  $0.187 \text{ cm}^3 \text{ cm}^{-3}$ , respectively, whereas values of  $0.0057 \text{ cm min}^{-1}$ ,  $70.1 \text{ cm}$ , and  $0.265 \text{ cm}^3 \text{ cm}^{-3}$  were used for wet soil samples. The details of the infiltration laboratory experiments for dry and wet soils are available in [34]. Another four 1D vertical infiltration data sets presented by Nie et al. [35] for clay loam and sandy loam were used in this study, and the infiltration time used was 60 min. During the infiltration process, the depth of ponding water was kept constant. The soil water characteristic curves and  $K_s$  were measured using a soil moisture suction meter (SXY-2, China) and an unsaturated hydraulic conductivity meter (FS-1, China), respectively. The value of  $\psi_m$  was determined using the method of Bautista et al. [29] according to the soil water characteristic parameters. Table 1 lists the details of the six laboratory experimental data sets.

**Table 1.** Details of six laboratory experimental data sets.

No.	Soil Texture	$\gamma_d$ (g $\text{cm}^{-3}$ )	$\theta_0$ ( $\text{cm}^3 \text{ cm}^{-3}$ )	$\theta_s$ ( $\text{cm}^3 \text{ cm}^{-3}$ )	$\Delta\theta$ ( $\text{cm}^3 \text{ cm}^{-3}$ )	$h_0$ (cm)	$\psi_m$ (cm)	$h_0 + \psi_m$ (cm)	$K_s$ (cm $\text{min}^{-1}$ )	$T$ (min)
L1	Clay	—	—	—	0.187	—	—	69.3	0.0039	70
L2		—	—	—	0.265	—	—	70.1	0.0057	80
L3	Clay	1.3	0.156	0.503	0.347	5.5	60.7	66.2	0.0133	60
L4	loam	1.4	0.168	0.433	0.265	10.5	17.1	27.6	0.0099	60
L5	Sandy	1.4	0.098	0.376	0.278	10.5	21.5	32.0	0.0559	60
L6	loam	1.5	0.135	0.355	0.220	5.5	30.2	35.7	0.0308	60

Notes:  $\gamma_d$ : bulk density;  $\theta_0$ : initial volumetric moisture content;  $\theta_s$ : saturation moisture content;  $\Delta\theta = \theta_s - \theta_0$ ;  $h_0$ : depth of ponding water;  $\psi_m$ : suction head at the wetting front;  $K_s$ : saturated hydraulic conductivity;  $t$ : infiltration time. L1 and L2: Fok and Chiang [34]. L1 is representative of dry soil, and L2 is representative of wet soil. Data that were not provided by Fok and Chiang are denoted by Fok and Chiang [34]. L3, L4, L5, and L6: Nie et al. [35].

### 3.2. Numerical Simulation

Numerical simulation is an appropriate approach for investigating the soil infiltration process, and it provides a more flexible representation of the flow domain, boundary conditions, and soil properties than field tests [36]. Typically, 1D vertical infiltration processes are simulated using HYDRUS-1D software [37]. Assuming homogeneous and isotropic soil, the governing equation for the water flow can be written as

$$\frac{\partial \theta}{\partial t} = \frac{\partial}{\partial z} \left[ K(h) \frac{\partial h}{\partial z} \right] - \frac{\partial K(h)}{\partial z} \quad (18)$$

where  $z$  is the vertical coordinate for which positive is taken to be downwards,  $\theta$  is the volumetric moisture content ( $\text{cm}^3 \text{cm}^{-3}$ ),  $h$  is the soil water pressure head (cm), and  $K(h)$  represents the unsaturated hydraulic conductivity ( $\text{cm min}^{-1}$ ).  $K(h)$  and  $S_e$ , which represent the soil water effective saturation, are described using the van Genuchten-Mualem model (VG-M model) [38] as follows:

$$K(h) = \begin{cases} K_s S_e^l \left[ 1 - (1 - S_e^{\frac{1}{m}})^m \right]^2 & h < 0 \\ K_s & h \geq 0 \end{cases} \quad (19)$$

$$S_e = \begin{cases} \frac{\theta - \theta_r}{\theta_s - \theta_r} = \frac{1}{(1 + |\alpha h|^n)^m} & h < 0 \\ 1 & h \geq 0 \end{cases} \quad (20)$$

where  $\theta_r$  is the residual soil water content ( $\text{cm}^3 \text{cm}^{-3}$ );  $m$ ,  $n$ ,  $a$ , and  $l$  are empirical shape parameters of the soil water characteristic curve; and  $m = 1 - 1/n$ . The initial and boundary conditions for the simulation of 1D vertical infiltration can be expressed as

$$\begin{cases} h(z, t) = h_n & 0 \leq z \leq Z, t = 0 \\ h = h_0 & t > 0, z = 0 \\ h = h_n & t > 0, z = Z \end{cases} \quad (21)$$

where  $h_n$  is the pressure head corresponding to the  $\theta_0$  condition (cm) and  $Z$  is the maximum vertical depth of the simulated domain;  $Z = 120$  cm was adopted in this study.

For a thorough test, the models were evaluated using the previously described data for six typical soils [39]. The soil water characteristic parameters were obtained from Carsel and Parrish [39], who studied six typical soils under different initial conditions. The VG-M model parameters of the six typical soils are listed in Table 2. Moreover, the initial conditions of the vertical infiltration were simulated using HYDRUS-1D and are listed in Table 3.

**Table 2.** Van Genuchten-Mualem (VG-M) model parameters of six typical soils (Carsel and Parrish [39]).

Soil Texture	$\theta_r$ ( $\text{cm}^3 \text{cm}^{-3}$ )	$\theta_s$ ( $\text{cm}^3 \text{cm}^{-3}$ )	$a$ ( $\text{cm}^{-1}$ )	$l$	$n$	$K_s$ ( $\text{cm min}^{-1}$ )
Sand	0.045	0.430	0.145	0.5	2.680	0.4950
Loam	0.078	0.430	0.036	0.5	1.560	0.0173
Silt	0.034	0.460	0.016	0.5	1.370	0.0042
Silt loam	0.067	0.450	0.020	0.5	1.410	0.0075
Clay loam	0.095	0.410	0.019	0.5	1.310	0.0043
Sandy loam	0.065	0.410	0.075	0.5	1.890	0.0740

Notes:  $\theta_r$ : residual soil water content;  $\theta_s$ : saturation moisture content;  $K_s$ : saturated hydraulic conductivity;  $l$  and  $n$ : empirical shape parameters of the soil water characteristic curve.

**Table 3.** Simulation of initial conditions of vertical infiltration using HYDRUS-1D.

No.	Soil Texture	$\theta_0$ (cm <sup>3</sup> cm <sup>-3</sup> )	$\Delta\theta$ (cm <sup>3</sup> cm <sup>-3</sup> )	$h_0$ (cm)	$\psi_m$ (cm)	$t$ (min)
S1	Sand	0.153	0.277	5	3.80	40
S2				10		
S3	Loam	0.157	0.273	5	6.92	900
S4				10		
S5	Silt	0.228	0.232	5	9.93	900
S6				10		
S7	Silt loam	0.125	0.325	5	8.95	1200
S8				10		
S9	Clay loam	0.172	0.238	5	6.86	1200
S10				10		
S11	Sandy loam	0.122	0.288	5	4.97	200
S12				10		

Notes:  $\theta_0$ : initial volumetric moisture content;  $\Delta\theta = \theta_s - \theta_0$ ;  $\theta_s$ : saturation moisture content;  $h_0$ : depth of ponding water;  $\psi_m$ : suction head at the wetting front;  $t$ : infiltration time.

### 3.3. Criteria for Model Evaluation

In this study, the performance of each model was evaluated by comparing the statistical indicators of the estimated values with the measured or simulated values obtained using HYDRUS-1D. The indicators used were the root mean square error (RMSE), the mean absolute percent relative error (MAPRE), and the percent bias (PB). These indicators can be calculated as follows [2,40,41]:

$$\text{RMSE} = \left[ \frac{1}{N} \sum_{i=1}^N (Z_{fei} - Z_{fmi}(f_{si}))^2 \right]^{0.5} \quad (22)$$

$$\text{MAPRE} = \frac{1}{N} \sum_{i=1}^N \left( \frac{|Z_{fei} - Z_{fmi}(f_{si})|}{Z_{fmi}(f_{si})} \times 100\% \right) \quad (23)$$

$$\text{PB} = \frac{\sum_{i=1}^N (Z_{fei} - Z_{fmi}(f_{si}))}{\sum_{i=1}^N Z_{fmi}(f_{si})} \times 100\% \quad (24)$$

where  $i$  is an integer varying from 1 to  $N$ ;  $N$  is the total number of data sets;  $Z_{fei}$  is the  $i$ th estimated value; and  $Z_{fmi}(f_{si})$  is the  $i$ th measured or simulated value. The RMSE, MAPRE, and PB provide a quantitative comparison of the estimated values with the measured or simulated values for the wetting front advancement depth. The RMSE provides an overall measure of the degree to which the data differ from the model estimations, whereas the PB is the deviation of the data being evaluated, expressed as a percentage [40]. The MAPRE is a measure of the accuracy of the models evaluated using the estimated and measured or simulated values. A lower RMSE and MAPRE indicate a favorable model fit [42,43]. If PB is less than  $\pm 10\%$ , the PB is considered to be within a very good range [40].

Additionally, the overall performance index (OPI) was used for a comprehensive evaluation of the four models on the basis of the three indicators. The OPI can be calculated as follows [2]:

$$\text{OPI} = \frac{1}{M} \sum_{p=1}^M \sum_{q=1}^K \text{RW}_q \quad (25)$$

where  $p = 1, 2, \dots, M$ , for which  $M$  is the number of total treatments for both laboratory experiments and simulations using HYDRUS-1D ( $M = 18$  in this study);  $q = 1, 2, \dots, K$ , for which  $K$  is the number

of indicators used to assess the accuracy of the models ( $K = 3$  in this study); and  $RW_q$  is the relative weight ( $RW$ ) of each model, which is estimated as the ratio of the assigned weight of an indicator to the rank of the model for the estimated  $Z_f$ , where the scope of  $RW_q$  is 0–1. In this study, more specifically, the first rank ( $RW = 1.0$ ) was assigned to the model with the lowest RMSE, MAPRE, or absolute PB. The fourth (last) rank ( $RW = 0.25$ ) was assigned to the model with the highest RMSE, MAPRE, or absolute PB. The second ( $RW = 0.75$ ) and the third ranks ( $RW = 0.50$ ) were assigned by order. Moreover, an equal weight coefficient of  $1/3$  (at an interval of  $1/3$ ) was assigned to the RMSE, MAPRE, and PB, making a total weight of 1.

#### 4. Results and Discussion

##### 4.1. Comparison of the Four Models Using Measured Values of $Z_f$

The wetting front depth  $Z_f$  was estimated using Equation (4) (GA model), Equation (9) (Stone model), Equation (10) (Ali model), and Equation (17) (proposed model), and  $K_s$ ,  $h_0 + \psi_m$ , and  $\Delta\theta$  were taken from Table 1. Subsequently, the estimated values were compared with the measured values. The results are presented in Figure 3 and in Table 4.

**Table 4.** Error analysis of measured and estimated wetting front depth  $Z_f$ .

No.	GA Model			Proposed Model			Ali Model			Stone Model		
	RMSE (cm)	MAPRE (%)	PB (%)	RMSE (cm)	MAPRE (%)	PB (%)	RMSE (cm)	MAPRE (%)	PB (%)	RMSE (cm)	MAPRE (%)	PB (%)
L1	0.47	3.17	3.55	0.34	2.87	2.60	0.64	6.73	−4.09	0.59	4.89	−5.26
L2	0.57	4.64	4.98	0.68	5.56	6.12	0.24	2.05	−0.59	0.37	2.75	−2.20
L3	1.26	6.46	−8.12	1.07	5.25	−6.74	1.81	10.96	−11.54	2.27	12.17	−15.19
L4	0.45	4.44	−3.41	0.35	3.40	−2.03	0.47	5.44	−4.90	1.18	9.04	−12.08
L5	1.53	6.17	−5.79	1.30	5.44	−4.74	1.45	5.41	−6.01	3.97	12.84	−15.85
L6	1.73	6.32	−7.61	1.49	5.89	−6.35	1.50	6.52	−7.11	3.76	13.33	−17.01
Mean value	1.00	5.20	−2.73	0.87	4.73	−1.86	1.02	6.18	−5.71	2.02	9.17	−11.27

Notes: GA model: Green-Ampt model; RMSE: root mean square error; MAPRE: mean absolute percent relative error; PB: percent bias.

As shown in Figure 3 and Table 4, the estimated  $Z_f$  obtained using the GA model, the proposed model, and the Ali model were in favorable agreement with the measured values. Table 4 presents the average RMSE, MAPRE and PB calculated for analyzing the measured and estimated values. The smallest RMSE value of 0.87 cm was found for the proposed model, followed by the GA model and the Ali model, both of which showed a value of approximately 1.0 cm. By contrast, the Stone model was found to have the largest RMSE value of 2.02 cm. The smallest MAPRE value of 4.73% was found for the proposed model, followed by the GA model and Ali model, which obtained values of 5.20% and 6.18%, respectively. By contrast, the Stone model was found to have the largest value of 9.17%. The best PB values were obtained for the proposed model and the GA model:  $-1.86\%$  and  $-2.73\%$ , respectively. The PB value of the Ali model ( $-5.71\%$ ) was approximately 3 times that of the proposed model, whereas the PB of the Stone model ( $-11.27\%$ ) was nearly 6 times that of the proposed model. Notably, the mean PBs of all the models were less than 0, indicating that the estimated values of  $Z_f$  obtained using the four models were slightly lower than the measured values. Two main reasons can explain the errors between the estimated  $Z_f$  obtained using the four models and the measured values. First, measurement errors are inevitable in laboratory experiments. Second, the estimated values of  $Z_f$  were obtained for infiltration in saturated soil, whereas transmission wetting zones exist under actual field conditions [44,45]. Generally, the proposed model, the GA model, and the Ali model estimated the  $Z_f$  value of 1D vertical infiltration with high accuracy, as indicated by their superior RMSE, MAPRE, and PB. The mean PBs had a magnitude of less than 6.00% for all six laboratory experimental data sets, which indicated a good consistency between the estimated and measured values [40].

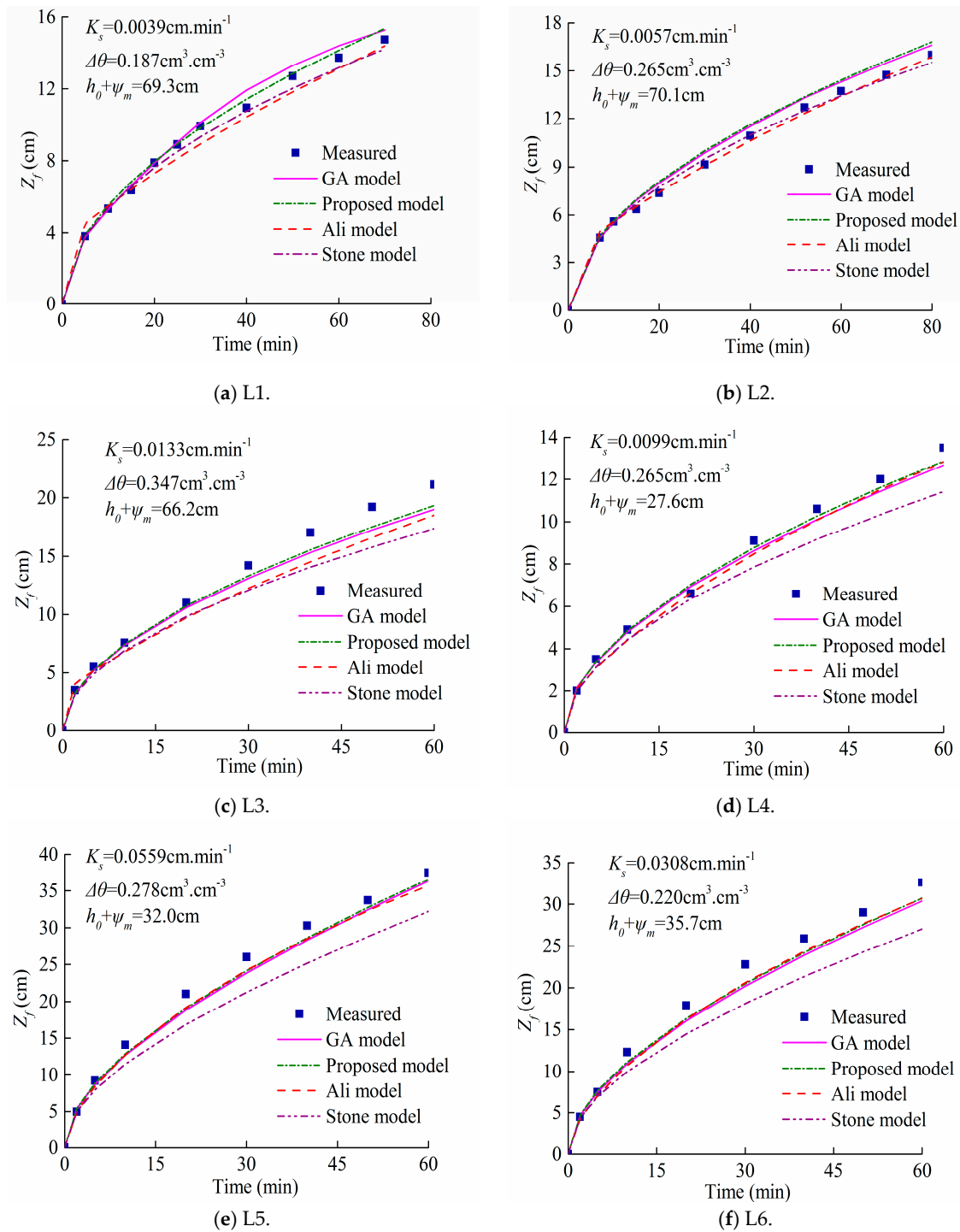


Figure 3. Comparison of estimated wetting front depth  $Z_f$  with measured values.

#### 4.2. Comparison of the Four Models Using HYDRUS-1D-Simulated Values of $Z_f$

To test the universality of the proposed model, HYDRUS-1D was used to simulate  $Z_f$  as a criterion, and the simulated values were compared with the estimated values obtained using the four models. The values of  $K_s$ ,  $h_0 + \psi_m$ , and  $\Delta\theta$  were taken from Tables 2 and 3. The results of the comparison of the simulated and estimated  $Z_f$  are provided in Figure 4 and in Table 5.

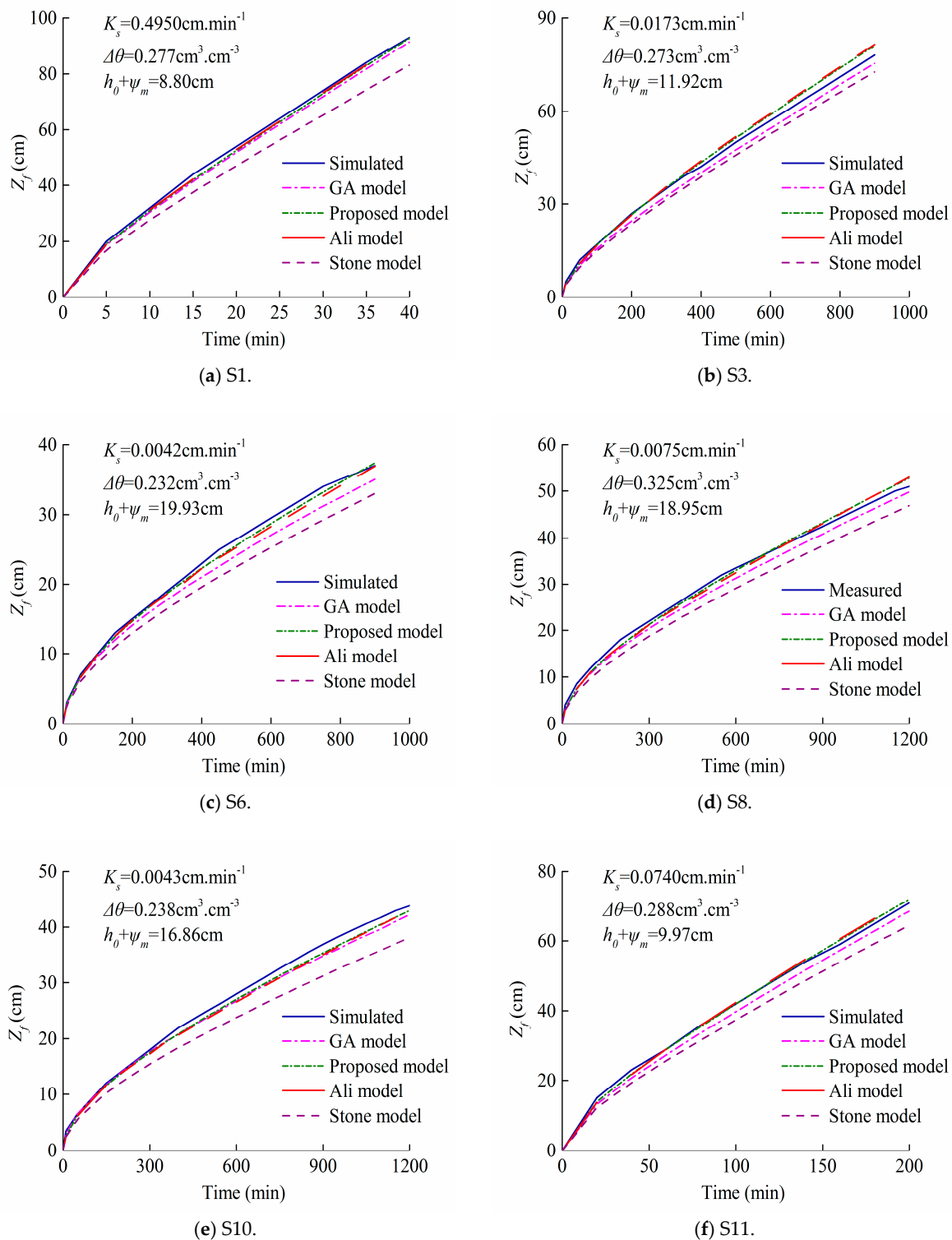


Figure 4. Comparison of estimated wetting front depth  $Z_f$  with HYDRUS-1D-simulated values.

As demonstrated in Figure 4 and Table 5, almost no differences were observed between the simulated values and all the estimated values obtained using the GA model, the proposed model, and the Ali model. The average RMSE, MAPRE, and PB are shown in Table 5. Among the four models, the accuracy of the proposed model was the highest, as indicated by the smallest RMSE, MAPRE, and PB values of 1.16 cm, 3.69%, and  $-1.26\%$ , respectively. The Ali model and the GA model were

ranked second and third in terms of their accuracy. The results showed that the accuracy of the Ali model was slightly higher than that of the GA model. For the Ali model and the GA model, the RMSEs were 1.31 cm and 2.13 cm, the MAPREs were 4.34% and 7.87%, and the PBs were  $-1.33\%$  and  $-6.10\%$ , respectively. The Stone model still had the largest values for all three indicators, almost 10 times those of the proposed model. The RMSE, MAPRE, and PB of the Stone model were 4.84 cm, 13.25%, and  $-12.31\%$ , respectively. Similarly, the mean PB of all the models was less than 0, indicating that the four models slightly underestimated  $Z_f$  compared with the simulated values (Table 5).

**Table 5.** Error analysis of HYDRUS-1D-simulated values and estimated wetting front depth  $Z_f$ .

No.	GA Model			Proposed Model			Ali Model			Stone Model		
	RMSE (cm)	MAPRE (%)	PB (%)	RMSE (cm)	MAPRE (%)	PB (%)	RMSE (cm)	MAPRE (%)	PB (%)	RMSE (cm)	MAPRE (%)	PB (%)
S1	1.98	4.16	-3.33	1.21	1.75	-1.91	0.99	2.07	-1.49	7.48	11.13	-12.26
S2	1.67	3.73	-1.97	1.58	2.52	-1.84	1.42	2.37	-1.30	8.12	12.84	-12.34
S3	2.26	6.49	-4.91	1.74	3.33	2.66	2.07	4.10	3.18	3.92	10.09	-8.39
S4	2.13	5.84	-4.16	0.97	2.86	0.46	1.38	3.64	0.94	5.56	11.41	-10.59
S5	3.09	17.36	-14.03	1.21	6.76	-4.28	1.35	7.64	-5.28	3.41	17.18	-15.55
S6	1.93	8.56	-7.43	0.58	2.51	-1.99	0.86	3.67	-3.16	3.44	13.58	-13.63
S7	2.06	10.21	-7.08	1.62	5.56	2.14	1.82	6.37	2.10	2.71	12.06	-9.43
S8	1.68	7.04	-5.17	0.89	3.84	-0.14	1.02	4.56	-0.77	3.80	13.46	-11.67
S9	3.24	13.95	-11.87	1.56	6.92	-5.90	1.59	7.56	-6.12	4.48	17.61	-16.69
S10	1.44	4.90	-4.56	1.07	4.39	-3.61	1.32	5.50	-4.45	4.40	15.51	-14.89
S11	2.15	6.31	-4.82	0.83	2.04	0.23	1.05	2.50	0.74	4.77	11.60	-10.50
S12	1.92	4.78	-3.84	0.70	1.77	-0.91	0.87	2.08	-0.37	6.03	12.57	-11.78
Mean value	2.13	7.78	-6.10	1.16	3.69	-1.26	1.31	4.34	-1.33	4.84	13.25	-12.31

Notes: GA model: Green-Ampt model; RMSE: root mean square error; MAPRE: means absolute percent relative error; PB: percent bias.

The main reason for the errors was that HYDRUS-1D uses finite elements to define the computational grid needed to solve Equation (18), and the finite element mesh is an important step when setting up a simulation. Thus, the simulated errors were caused by the spatial discretization of the computational domain. Moreover, the assumption of saturated zones in the four models was another reason for the errors. Transmission wetting zones, rather than saturated zones, exist under actual field conditions [44,45]. Overall, however, the four models can reliably estimate the  $Z_f$  for 1D vertical infiltration.

#### 4.3. Comparison and Discussion of the Four Models

The OPI was calculated using Equation (25) on the basis of the values in Tables 4 and 5. The results revealed that the proposed model had the highest performance, as indicated by the highest OPI of 0.926. The Ali model and the GA model were ranked second and third, and had OPIs of 0.736 and 0.546, respectively. The Stone model was ranked fourth, having the lowest OPI of 0.292. On the basis of these OPIs and considering each model's numerical accuracy, the four models were ranked as follows: proposed model > Ali model > GA model > Stone model. It can be concluded that the proposed model exhibited the highest performance for estimating  $Z_f$ , followed by the Ali model, the GA model, and the Stone model.

The GA model is an analytical solution derived from Darcy's equation once some assumptions have been made, and it is derived indirectly through Richards's model with some simplification [12]. The assumptions and simplification may have caused errors in the estimation of  $Z_f$ . According to comparisons of the estimated values with the measured and simulated values, the largest RMSE, MAPRE, and PB values were 3.24 cm, 17.36%, and  $-14.03\%$ , respectively, for the GA model (Tables 4 and 5). These results indicated that the GA model can reliably estimate  $Z_f$  with high accuracy, although its estimated value is slightly higher than that of the proposed model. However, the GA model is expressed by an implicit equation and is solved using an iterative method, which, to a certain extent, limits the application of the model [7,13,14].

In the Ali model, the logarithmic term of the GA model (Equation (4)) is replaced by a sequential segmental second-order polynomial; subsequently, a generalized algebraic equation-based model is developed to estimate the  $Z_f$  value of 1D vertical infiltration [27]. According to comparisons of the estimated values with the measured and simulated values, the largest RMSE, MAPRE, and PB values were 2.07 cm, 10.96%, and  $-11.54\%$ , respectively, for the Ali model (Tables 4 and 5). The accuracy of the Ali model was almost consistent with that of the proposed model and it was even slightly higher than that of the GA model. This finding indicated the reliability of the Ali model for estimating the  $Z_f$  value of 1D vertical infiltration. Nonetheless, the Ali model is complex to employ, as  $Z_f$  is estimated in three steps [27]. First, the periods are determined for different infiltration segments. Second, the three parameters  $F_1$ ,  $F_2$ , and  $F_3$  in Equation (10) are selected according to different infiltration segments. Finally, the values of  $Z_f$  can be estimated using Equation (10).

The results in Tables 4 and 5 indicated that among the four models, the Stone model produced the largest errors. According to comparisons of the estimated values with the measured and simulated values, the largest RMSE, MAPRE, and PB values were 8.12 cm, 17.61%, and  $-17.01\%$ , respectively, for the Stone model. The development of the Stone model is similar to the form of Philip's equation [30]. In the Stone model, it is assumed that the steady infiltration rate in Philip's equation is equal to the saturated conductivity,  $K_s$ , which is inconsistent with actual conditions. As suggested by some researchers, the steady infiltration rate can be arranged from 1/3 to 2/3 of  $K_s$  [23–26]. Thus, the unreasonable assumption leads to inaccuracy in the Stone model. Although an error term was added to account for the error in the approximation of the Stone model, this term did not effectively compensate for the errors generated from the unreasonable assumption.

The model proposed in this study for estimating the  $Z_f$  value of 1D vertical infiltration is based on the two-parameter linearized infiltration equation developed by Valiantzas (Equation (11)) [31]. The ratio of the steady infiltration rate to  $K_s$  was 0.5 in the study of Valiantzas [31], which may be assumed to typically represent the infiltration behavior of many natural soils under ponding water. Additionally, Valiantzas selected 10 types of soil for verification, and the results showed that Valiantzas's equation was more appropriate than other two- or three-parameter nonlinear infiltration equations [31]. Thus, when developing the proposed model, an error term was added to the model to compensate for the errors caused by the Taylor series expansion of Valiantzas's equation. From Tables 4 and 5, according to comparisons of the estimated values with the measured and simulated values, the largest RMSE, MAPRE, and PB values were 1.74 cm, 6.92%, and  $-6.74\%$ , respectively, for the proposed model. These results indicated that among the four models, the proposed model exhibited the highest accuracy, demonstrating its reliability for estimating the  $Z_f$  value of 1D vertical infiltration. Moreover, the proposed model was developed by adopting 0–20 as the range for the dimensionless depth of the advancement of the wetting front,  $L^*$ , although  $L^*$  theoretically ranges from 0 to  $+\infty$ , according to Equation (6). The adopted range is suitable for estimating the  $Z_f$  value of 1D vertical infiltration under surface irrigation. However, the accuracy of the proposed model may decrease when  $L^*$  is greater than 20.

## 5. Conclusions

The approximate explicit solution to the GA model proposed in this study can be used to estimate the wetting front depth of 1D vertical infiltration. The resulting approximate equation is based on the two-parameter infiltration equation developed by Valiantzas [31], and the proposed model includes an error term to account for the approximation.

The proposed model, the GA model, the Ali model, and the Stone model were validated and evaluated using measured values derived from laboratory experiments and simulated values obtained using HYDRUS-1D. The RMSE, MSPRE, and PB were used as indicators to evaluate the accuracy of the four models. The results indicated that the proposed model is more convenient than the GA model and the Ali model. Moreover, according to comparisons of the estimated values with the measured and simulated values, the proposed model had the smallest RMSE, MSPRE, and PB values.

Furthermore, the proposed model had the highest OPI of 0.926. Thus, this model showed the highest performance for estimating the  $Z_f$  value of 1D vertical infiltration. The Ali model, the GA model, and the Stone model were ranked second, third, and fourth, respectively, and had OPIs of 0.736, 0.546, and 0.292, respectively.

**Acknowledgments:** This research was jointly supported by grants from the Natural Science Foundation of China (51579205), the National Program on Key Research Projects during the 13th Five-Year Plan Period (2016YFC0400203), the Natural Science Foundation of Shaanxi Province (2016JM5053), the Scientific Research Program funded of Shaanxi Provincial Education Department (15JS064), and the Special Fund for Agro-scientific Research in the Public Interest (No. 201503124).

**Author Contributions:** Wei-Bo Nie and Yi-Bo Li analyzed the data and wrote the paper. Wei-Bo Nie and Xiao-Yi Ma contributed reagents, materials, and analysis tools. Xiao-Yi Ma and Liang-Jun Fei revised the paper.

**Conflicts of Interest:** The authors declare no conflict of interest.

## References

- Mishra, S.K.; Tyagi, J.V.; Singh, V.P. Comparison of infiltration models. *Hydrol. Process.* **2003**, *17*, 2629–2652. [[CrossRef](#)]
- Ali, S.; Islam, A.; Mishra, P.K.; Sikka, A.K. Green-Ampt approximations: A comprehensive analysis. *J. Hydrol.* **2016**, *535*, 340–355. [[CrossRef](#)]
- Hu, H.P.; Gao, L.; Tian, F.Q. Empirical equation for development of soil wetted body under surface drip irrigation condition. *J. Tsinghua Univ. Sci. Technol.* **2010**, *50*, 839–843.
- Nie, W.B.; Ma, X.Y.; Wang, S.L. Forecast model for wetting front migration distance under furrow irrigation infiltration. *Trans. Chin. Soc. Agric. Eng.* **2009**, *25*, 20–25.
- Xiong, Y.W.; Furman, A.; Wallach, R. Moment analysis description of wetting and redistribution plumes in wettable and water-Repellent soils. *J. Hydrol.* **2012**, *422*, 30–42. [[CrossRef](#)]
- Zhang, Y.Y.; Zhao, X.N.; Wu, P.T. Soil wetting patterns and water distribution as affected by irrigation for uncropped ridges and furrows. *Pedosphere* **2015**, *25*, 468–477. [[CrossRef](#)]
- Rao, M.D.; Raghuwanshi, N.S.; Singh, R. Development of a physically based 1D-Infiltration model for seal formed irrigated soils. *Agric. Water Manag.* **2006**, *84*, 164–174.
- Valiantzas, D.; Pollalis, E.D.; Soulis, K.X.; Londra, P.A. Rapid graphical detection of weakness problems in numerical simulation infiltration models using a linearizes form equation. *J. Irrig. Drain. Eng. ASCE* **2011**, *137*, 524–529. [[CrossRef](#)]
- Malek, K.; Peters, R.T. Wetting pattern models for drip irrigation: New empirical model. *J. Irrig. Drain. Eng. ASCE* **2011**, *137*, 530–536. [[CrossRef](#)]
- Rasheeda, S.; Sasikumar, K. Modelling vertical infiltration in an unsaturated porous media using neural network architecture. *Aquat. Procedia* **2015**, *4*, 1008–1015. [[CrossRef](#)]
- Green, W.H.; Ampt, G. Study on soil physics-1. The flow of air and water through soils. *J. Agric. Sci.* **1911**, *4*, 1–24.
- Philip, J. Plant water relations: Some physical aspects. *Annu. Rev. Plant Physiol.* **1966**, *17*, 245–268. [[CrossRef](#)]
- Stone, J.J.; Hawkins, R.H.; Shirley, E.D. Approximate form of Green-Ampt infiltration equation. *J. Irrig. Drain. Eng. ASCE* **1994**, *120*, 128–137. [[CrossRef](#)]
- Enciso-Medina, J.; Martin, D.; Eisenhauer, D. Infiltration model from furrow irrigation. *J. Irrig. Drain. Eng. ASCE* **1998**, *124*, 73–80. [[CrossRef](#)]
- Li, R.M.; Steven, M.A.; Simons, D.B. Solutions to Green-Ampt infiltration equation. *J. Irrig. Drain. Eng. Div. ASCE* **1976**, *102*, 239–248.
- Salvucci, G.D.; Entekhabi, D. Explicit expressions for Green-Ampt (delta function diffusivity) infiltration rate and cumulative storage. *Water Resour. Res.* **1994**, *30*, 2661–2663. [[CrossRef](#)]
- Barry, D.A.; Parlange, J.Y.; Sander, G.C.; Sivapalan, M. Comment on explicit expression for Green-Ampt (delta function diffusivity) infiltration rate and cumulative storage. *Water Resour. Res.* **1995**, *31*, 1445–1446. [[CrossRef](#)]
- Serrano, S.E. Explicit solution to Green and Ampt infiltration equation. *J. Hydrol. Eng.* **2001**, *6*, 336–340. [[CrossRef](#)]
- Chen, L.; Young, M.H. Green-Ampt infiltration model for sloping surfaces. *Water Resour. Res.* **2006**, *42*, 887–896. [[CrossRef](#)]

20. Mailapalli, D.R.; Wallender, W.W.; Singh, R.; Raghuwanshi, N.S. Application of a nonstandard explicit integration to solve Green and Ampt infiltration equation. *J. Hydrol. Eng.* **2009**, *14*, 203–206. [[CrossRef](#)]
21. Almedeij, J.; Esen, I.I. Modified Green-Ampt infiltration model for steady rainfall. *J. Hydrol. Eng.* **2014**, *19*, 04014011. [[CrossRef](#)]
22. Zhu, J.T.; Ogden, F.L.; Lai, W.C.; Chen, X.F.; Talbot, C.A. An explicit approach to capture diffusive effects in finite water-Content method for solving vadose zone flow. *J. Hydrol.* **2016**, *535*, 270–281. [[CrossRef](#)]
23. Youngs, E.G. An estimation of sorptivity for infiltration studies from moisture moments considerations. *Soil Sci.* **1968**, *106*, 157–163. [[CrossRef](#)]
24. Philip, J.R. Theory of infiltration. *Adv. Hydrosci.* **1969**, *5*, 215–296.
25. Talsma, T.; Parlange, J.Y. One-Dimensional vertical infiltration. *Aust. J. Soil Res.* **1972**, *10*, 143–150. [[CrossRef](#)]
26. Fuentes, C.; Haverkamp, R.; Parlange, J.Y. Parameter constraints on closedform soil-Water relationships. *J. Hydrol.* **1992**, *134*, 117–142. [[CrossRef](#)]
27. Ali, S.; Ghosh, N.C.; Singh, R.; Sathy, B.K. Generalized explicit models for estimation of wetting front length and potential recharge. *Water Resour. Manag.* **2013**, *27*, 2429–2445. [[CrossRef](#)]
28. Bouwer, H. *Groundwater Hydrology*, 1st ed.; Wiley: New York, NY, USA, 1978.
29. Bautista, E.; Warrick, A.W.; Strelkoff, T.S. New results for an approximate method for calculating two-Dimensional furrow infiltration. *J. Irrig. Drain. Eng. ASCE* **2014**, *140*, 04014032. [[CrossRef](#)]
30. Philip, J.R. The theory of infiltration: 4. Sorptivity and algebraic infiltration equations. *Soil Sci.* **1957**, *84*, 257–264. [[CrossRef](#)]
31. Valiantzas, J.D. New linearized two-parameter infiltration equation for direct determination of conductivity and sorptivity. *J. Hydrol.* **2010**, *384*, 1–13. [[CrossRef](#)]
32. Esfandiari, M.; Maheshwari, B.L. Field values of shape factor for estimating surface storage in furrows on a clay soil. *Irrig. Sci.* **1997**, *17*, 157–161. [[CrossRef](#)]
33. Nie, W.B.; Fei, L.J.; Ma, X.Y. Impact of infiltration parameters and Manning roughness on the advance trajectory and irrigation performance for closed-end furrows. *Span. J. Agric. Res.* **2014**, *12*, 1180–1191. [[CrossRef](#)]
34. Fok, Y.S.; Chiang, H.S. 2-D infiltration equations for furrow irrigation. *J. Irrig. Drain. Div. ASCE* **1984**, *110*, 209–217. [[CrossRef](#)]
35. Nie, W.B.; Ma, X.Y.; Wang, S.L. Numerical simulation of one-dimensional soil infiltration characteristic. *J. Irrig. Drain. Eng.* **2009**, *28*, 53–57.
36. Warrick, A.W. *Soil Water Dynamics*; Oxford University Press: New York, NY, USA, 2003.
37. *HYDRUS-1D*, version 4.0; PC-Progress: Prague, Czech Republic, 2007.
38. Van Genuchten, M.Th. A closed-form equation for predicting the hydraulic conductivity of unsaturated soils. *Soil Sci. Soc. Am. J.* **1980**, *44*, 892–898. [[CrossRef](#)]
39. Carsel, R.F.; Parrish, R.S. Developing joint probability distributions of soil water retention characteristics. *Water Resour. Res.* **1988**, *24*, 755–769. [[CrossRef](#)]
40. Moriasi, D.; Arnold, J.; Liew, M.W.V.; Veith, T.L. Model evaluation guidelines for systematic quantification of accuracy in watershed simulations. *Trans. Am. Soc. Agric. Biol. Eng.* **2007**, *50*, 885–900. [[CrossRef](#)]
41. Zhang, Y.Y.; Wu, P.T.; Zhao, X.N.; Wang, Z.K. Simulation of soil water dynamics for uncropped ridges and furrows under irrigation conditions. *Can. J. Soil Sci.* **2013**, *93*, 85–98. [[CrossRef](#)]
42. Jacovides, C.P.; Kontoyiannis, H. Statistical procedures for the evaluation of evapotranspiration computing models. *Agric. Water Manag.* **1995**, *27*, 365–371. [[CrossRef](#)]
43. Nayak, P.C.; Sudheer, K.P.; Rangan, D.M.; Ramasastri, K.S. A neuro-fuzzy computing technique for modelling hydrological time series. *J. Hydrol.* **2004**, *291*, 52–66. [[CrossRef](#)]
44. Ma, J.J.; Sun, X.H.; Guo, X.H. Varying head infiltration model based on Green-Ampt model and solution to its key parameters. *J. Hydrol. Eng.* **2010**, *41*, 61–67.
45. Mao, L.L.; Lia, Y.Z.; Hao, W.P.; Zhou, X.N.; Xu, C.Y.; Lei, T.W. A new method to estimate soil water infiltration based on a modified Green-Ampt model. *Soil Tillage Res.* **2016**, *161*, 31–37. [[CrossRef](#)]

